Am J Transl Res 2018;10(4):1172-1183
www.ajtr.org /ISSN:1943-8141/AJTR0069606

Original Article

MiR-101 inhibits the proliferation and metastasis of lung cancer by targeting zinc finger E-box binding homeobox 1

Le Han[1,2*], Wenjuan Chen[1,2*], Yanmin Xia[1], Yangrong Song[1], Zheng Zhao[1], Hao Cheng[1], Tao Jiang[1]

[1]Department of Thoracic Surgery, Tangdu Hospital, The Fourth Military Medical University, Xi'an 710038, Shaanxi, China; [2]Department of Thoracic Surgery, Tumor Hospital of Shaanxi Province, Xi'an 710038, Shaanxi, China. [*]Equal contributors.

Received November 22, 2017; Accepted February 7, 2018; Epub April 15, 2018; Published April 30, 2018

Abstract: MicroRNAs (miRNAs) are involved in the development and progression of lung cancer. MicroRNA-101 (miR-101) displays crucial properties in non-small cell lung cancer (NSCLC) by negatively regulating cell proliferation and invasion, but the underlying molecular mechanisms remain largely unknown. In this study, we found that miR-101 was underexpressed while zinc finger E-box binding homeobox 1 (ZEB1) was highly upregulated in NSCLC tissues and cells. The downregulation of miR-101 was positively associated with lymph node metastasis and poor prognosis of NSCLC patients. Dual-luciferase reporter assay showed that miR-101 directly targeted ZEB1 in NSCLC cells. Enforced expression of miR-101 significantly inhibited NSCLC cell proliferation, apoptosis resistance, migration, and invasion in vitro, which were attenuated by ZEB1 overexpression and phenocopied by ZEB1 knockdown, respectively. Consistently, miR-101 retarded NSCLC growth and metastasis in vivo. The findings indicated that miR-101 suppressed NSCLC growth and metastasis by targeting ZEB1, thereby providing new evidence of miR-101 as a potential therapeutic target for NSCLC patients.

Keywords: MicroRNA-101, lung cancer, proliferation, metastasis, zinc finger E-box binding homeobox 1

Introduction

Lung cancer is the leading cause of cancer-related deaths worldwide. It is the first most common malignancy in men and the fourth most common cancer in women [1]. Globally, lung cancer is the largest contributor to new cancer diagnoses (1.825 million new cases and 12.9% of total new cancer cases) and to death from cancer (1.59 million deaths and 19.4% of total cancer deaths) [2]. In China, about 733,300 new lung cancer cases and 610,200 deaths occurred [3]. Non-small cell lung cancer (NSCLC), the major type of lung cancers, accounts for 85% of all lung cancer cases, with a low five-year survival rate [4]. Although various therapeutic techniques have been developed, most patients have died because of insufficient NSCLC-specific biomarkers and tools for diagnosis and therapy [5]. The successful reduction of lung cancer mortality requires a thorough understanding of the biological process of NSCLC and some novel therapeutic strategies.

MicroRNAs (miRNAs) are small RNA molecules (21-23 nt) that act as negative regulators of gene expression by blocking mRNA translation or degradation of the target mRNAs [6, 7]. Aberrant miRNA expression has been observed in many types of human cancers, including lung cancer [8, 9]. Dysregulation of miRNAs is involved in the growth, metastasis, and multidrug resistance of NSCLC [10-12]. Reportedly, miR-101 exerts tumor-suppressive effects in multiple malignancies, including NSCLC [13-16]. Downregulation of miR-101 promotes epithelial to mesenchymal transition (EMT) in cisplatin-resistant NSCLC cells [15]. MiR-101 inhibits cell proliferation and invasion and enhances paclitaxel-induced apoptosis in NSCLC cells by directly targeting enhancer of zeste homolog 2 (EZH2) [16]. However, the molecular mechanisms of miR-101-repressed NSCLC remain largely unclear.

Zinc finger E-box binding homeobox 1 (ZEB1) belongs to the ZEB family of transcription factors,

which is characterized by a centrally located homeodomain and two zinc finger clusters responsible for DNA binding [17]. ZEB1 has been recognized as an important oncogene in a number of malignancies and may serve as a prognostic indicator for tumor patients [18-21]. Given the pivotal role of ZEB1 in the downregulation of E-cadherin, ZEB1 acts as a driver of EMT and cancer progression [22, 23]. EMT is a complex process to promote cancer metastasis in which epithelial cells acquire the characteristics of invasive mesenchymal cells [24]. Interestingly, ZEB1 mediates miRNA-elicited reduction in the proliferation, migration, invasion, and EMT of NSCLC cells [25-27]. Nevertheless, the biological functions and underlying mechanism by which ZEB1 involved in the growth and metastasis of NSCLC is unknown.

In this study, we revealed that miR-101 was downregulated while ZEB1 was upregulated in NSCLC tissue specimens and cell lines. Dual-luciferase assay results confirmed ZEB1 as a direct target of miR-101. Moreover, miR-101 dramatically repressed the proliferative, migratory, and invasive abilities of NSCLC cells in vitro; however, ectopic expression of ZEB1 reversed the inhibitory effects. In vivo, miR-101 restrained NSCLC growth and metastasis. Overall, these results provide persuasive evidence that miR-101 functions as a tumor suppressor and may be a possible therapeutic target in NSCLC.

Materials and methods

Clinical samples

Lung cancer and corresponding adjacent tissue specimens were obtained from NSCLC patients without chemotherapy or radiotherapy prior to surgery, who underwent curative resection at the Department of Thoracic Surgery, Tangdu Hospital, the Fourth Military Medical University between 2008 and 2011. Fresh samples were collected at the time of surgery, and were rapidly frozen in liquid nitrogen and stored at -80°C until use. All the patients were followed-up to 2016 or until death. Informed consent was signed by each patient. This study was approved by the Ethics Committee of Tangdu Hospital.

Cell culture

Human NSCLC cell lines (A549, H1299, H1650, and H1975) and an immortalized and non-tumorigenic human bronchial epithelial cell line NL20 were purchased from American Type Culture Collection (Manassas, VA, USA). The cell lines were authenticated by DNA (STR) profiling analysis, and were used no later than 6 months after receipt. All the cells were cultured in Roswell Park Memorial Institute 1640 (RPMI 1640; Gibco, Carlsbad, CA, USA) supplemented with penicillin (100 U/mL), streptomycin (100 U/mL) (Sigma-Aldrich, St. Louis, MO, USA), and 10% fetal bovine serum (FBS; Gibco) at 37°C in 5% CO_2.

Establishment of A549-luciferase (luc) cell line

To establish A549-luc cell line, lentivirus pLV-luc (Inovogen Biotechnology, Delhi, India) was used to infect A549 cells. After screening with puromycin (200 μg/mL; Sigma) for 16 days, the single clone stably expressed luciferase was obtained and named A549-luc cell line.

Plasmid and lentivirus constructs

The luciferase-3'-UTR-wild-type (WT) reporter or luciferase-3'-UTR-mutant (MUT) plasmids were prepared by inserting the ZEB1-3'-UTR-WT with a putative miR-101 binding site or its mutant sequence into the pGL3-control plasmid (Promega, Madison, WI, USA). The pUNO1-hZEB1 (open reading frame) plasmid was purchased from InvivoGen (Hong Kong, China). All constructs were confirmed by DNA sequencing. For the lentiviral expression of miR-101, complementary DNA strands corresponding to the pre-miR-101 sequence were synthesized and cloned into the *Age*I/*Eco*RI sites of pGCsi-H1-CMV-GFP (GeneChem, Shanghai, China). The constructs were co-transfected into A549 cells with the pMD2.G and psPAX2 packaging plasmids. After 48 h of transfection, the supernatant was collected, centrifuged, filtered, and used for the infection of A549 cells. A short hairpin RNA (shRNA) was designed based on the ZEB1 sequence, and a scrambled shRNA was used as a control. Paired deoxyribonucleotide oligos encoding the shRNAs were synthesized, annealed, and cloned into the *Eco*RI/*Nco*I sites of the pLKO.1 vector (Addgene, Cambridge, MA, USA). The constructs were co-transfected with the pCMV-VSVG and pCMV-bA.9 packaging plasmids into A549 packaging cells. The viral supernatants were harvested, filtered, and infected A549 cells. Cells were selected with 5 μg/mL puromycin (Sigma) to generate stable shRNA-expressing clones.

Cell transfection

The miR-101 and its negative control (miR-NC) mimics were synthesized by RiboBio (Guangzhou, China) and transfected using Lipofectamine 2000 reagent (Invitrogen, Carlsbad, CA, USA) according to the manufacturer's instructions. After cell confluence reached 80%, the indicated concentration of miR-101 or miR-NC mimics was transfected into A549 cells.

Dual-luciferase reporter assay

MiR-101 or miR-NC mimics was co-transfected with Plasmid pGL3-ZEB1-3'-UTR-WT or pGL3-ZEB1-3'-UTR-MUT into A549 cells. Dual-luciferase reporter assay (Promega) was conducted at 48 h after transfection. *Renilla* luciferase was co-transfected as a control for normalization.

Quantitative real-time polymerase chain reaction (qPCR)

For RNA extraction, the fresh tissues and cells were lysed with TRIzol reagent (Invitrogen) and purified using an RNeasy Mini Kit (Qiagen). Complementary DNA was synthesized using reverse transcriptase (Epicentre, Madison, WI, USA) or the miScript Reverse Transcription Kit (Qiagen) and then amplified using SYBR Premix Ex *Taq*™ (TaKaRa, Otsu, Shiga, Japan). The expression levels of mRNAs and miRNA were determined using the $2^{-\Delta\Delta Ct}$ method, with glyceraldehyde-3-phosphate dehydrogenase (GAPDH) and U6 as the internal controls, respectively. The primers used for PCR amplification are listed as follows: for ZEB1, 5'-AGAGCAGTGAAAG AGAAGGGAATGC-3' (forward) and 5'-GGTCCTCTTCAGGTGCCTCAG-3' (reverse); for GAPDH, 5'-TGCACCACCAACTGCTTAGC-3' (forward) and 5'-GGC ATGGACTGTGGTCATGAG-3' (reverse); for miR-101, 5'-CGGCGGTACAGTACT GTGATAA-3' (forward) and 5'-CTGGTGTCGTGGAGT CGGCAATTC-3' (reverse); and for U6, 5'-CTCGCTTCGGCAGCACA-3' (forward) and 5'-AACGCTTCACGAA TTTGCGT-3' (reverse).

Western blot analysis

Total proteins were extracted from fresh tissues and cells using RIPA buffer (Beyotime, China), resolved by 10% sodium dodecyl sulfate-polyacrylamide gel electrophoresis and electrophoretically transferred onto nitrocellulose membranes (Millipore, Bedford, MA, USA). The membranes were blocked for 1 h with 5% skim milk dissloved in Tris-phosphate buffer containing 0.05% Tween 20, and then incubated with the primary antibodies targeting ZEB1, Cyclin D1, Rb (all from Cell Signaling Technology, Danvers, MA, USA), Bcl-2, Bax, caspase-3, cleaved (cl)-caspase-3 (all from Abcam, Cambridge, UK), E-cadherin, Vimentin, and β-actin antibodies (all from Santa Cruz) at 4°C overnight. After 1h of incubation with the appropriate horseradish peroxidase-conjugated secondary antibody, the bands were detected by an enhanced chemiluminescence kit (Santa Cruz).

Cell viability assay

3-(4,5-dimethylthiazol-2-yl)-2,5-diphenyltetrazolium bromide (MTT; Sigma) assay was conducted to determine cell viability. Briefly, A549 cells were seeded into 96-well plates at a density of 5×10^3 cells/mL and transfected with the miR-101 mimic, miR-NC, or miR-101 mimic + ZEB1 plasmid. At 24 h after transfection, the cultures were continued for 24, 48, 72, and 96 h. At each time point, 25 μL of MTT (10 mg/mL, Sigma) was added to each well and successively incubated for 4 h at 37°C. After removing the supernatant, 200 μL of dimethyl sulfoxide (Invitrogen) was added to dissolve the formazan crystals for 30 min. The absorbance at 490 nm was measured with a microplate reader (Molecular Devices, Sunnyvale, CA, USA).

Colony formation assay

Cell proliferation was determined by colony formation assay. Briefly, at 24 h after transfection, 1×10^3 A549 cells were seeded into a six-well plate and the medium was refreshed every two days. After incubation for 14 days, the colonies were fixed with methanol and stained with 1% crystal violet for 15 min before being counted.

Apoptosis by flow cytometry

Flow cytometry was performed to measure cell apoptosis. In brief, A549 cells were harvested at 48 h post-transfection and were resuspended in 1 × binding buffer at a density of 1×10^6 cells/mL. After double staining with Annexin V-fluorescein isothiocyanate (FITC) for 15 min at 37°C and propidium iodide (PI) for 30 min in the dark using the Annexin V-FITC Apoptosis Detection Kit I (BestBio, Shanghai, China), the

cells were analyzed using a FACScan® flow cytometer equipped with Cell Quest software (BD Biosciences, San Jose, CA, USA).

Terminal transferase-mediated dUTP nick end labeling (TUNEL) assay

Tissue samples were collected and sectioned for TUNEL assay (Boster Biological Technology, Ltd., Wuhan, China) according to the manufacturer's instructions. Briefly, after deparaffinization and rehydration, sections were treated with proteinase K (Boster Biological Technology) for 20 min at room temperature. After rinsing, the sections were incubated with TUNEL reaction mixture at 37°C for 60 min. Slides were then mounted and observed under a fluorescence microscope (Olympus). Negative control slides were incubated with a labeling solution (without terminal transferase) instead of the TUNEL reaction mixture. The percentage of apoptotic cells was calculated with ImageJ (NIH Image, USA).

Enrichment factor assay

Cell apoptosis was evaluated by using the Cell Death Detection ELISA Plus Kit (Roche Applied Science, Mannheim, Germany), as per the instruction of manufacturer. The relative amounts of mono- and oligonucleosomes generated from the apoptotic cells were quantified using monoclonal antibodies directed against DNA and histones by ELISA. In brief, at 24 h after transfection, cytoplasmic fraction of the cells were transferred onto a streptavidin-coated plate and incubated for 2 h at room temperature with a mixture of peroxidase conjugated anti-DNA and biotin-labeled anti-histone. The plate was washed and incubated with 2,2'-azino-bis(3-ethylbenzothiazoline-6-sulfonic acid) diammonium salt. The absorbance was measured using a microplate reader (Molecular Devices) at 490 nm and normalized to miR-NC-transfected cells.

Caspase-3 activity assay

Caspase-3 activity was assessed the Caspase-3 Activity Assay Kit (Nanjing Jiancheng Bioengineering Institute, Nanjing, China) in accordance with the manufacturer's instructions. At 24 h after transfection, the cells were lyzed by using cell lysis buffer (Nanjing Jiancheng Bioengineering Institute) followed by shaking for 30 min at room temperature. After centrifugation at 800 *g* for 10 min, 100 μL of supernatant was transferred to another plate followed by incubation at 37°C with 100 μL of Ac-DEVD-pNA, a caspase-3 substrate. The absorbance was measured using a microplate reader (Molecular Devices) at 405 nm.

Wound-healing assay

Cell motility was measured by wound-healing assay. In brief, at 24 h after transfection, 1×10^6 A549 cells were seeded in a 6-cm dish. The cell monolayer was scraped in a straight line with a P200 pipet tip when the cells grew to 70% confluence. Photographs were taken at 0 h and 24 h after scratch using a phase-contrast microscope (Olympus, Tokyo, Japan). Gap width was analyzed with ImageJ (NIH). Gap width at 0 h was set to 100%.

Migration and invasion assay

Cell migration assay was performed using Transwell cell culture inserts (8-μm pore size, BD Biosciences), whereas invasion assay was conducted using a Transwell system with a matrigel-coated polycarbonate membrane. After cells undergoing serum starvation for 24 h, 1×10^5 A549 cells/100 μL were seeded in the upper chamber and incubated with RPMI 1640 containing 1% FBS. The bottom chamber was filled with RPMI 1640 containing 10% FBS. The transfected cells were allowed to migrate or invade for 12 h. The cells that migrated and invaded into the bottom of the inserts were stained with 4',6-diamidino-2-phenylindole (Sigma), visualized under an inverted microscope (Olympus), and then counted.

Animals

Six-week-old male severe combined immunodeficiency (SCID) mice were purchased from the Institute of Laboratory Animal Science, Chinese Academy of Medical Sciences (Beijing, China). The animals were bred under aseptic conditions and maintained in a facility with constant humidity and temperature (25°C-28°C) under a 12 h light/dark cycle. The experiments were approved by the Animal Care and Use Committee of Tangdu Hospital.

In vivo experiments

NSCLC xenografts were established by subcutaneously injecting 1×10^6 A549-luc cells, whi-

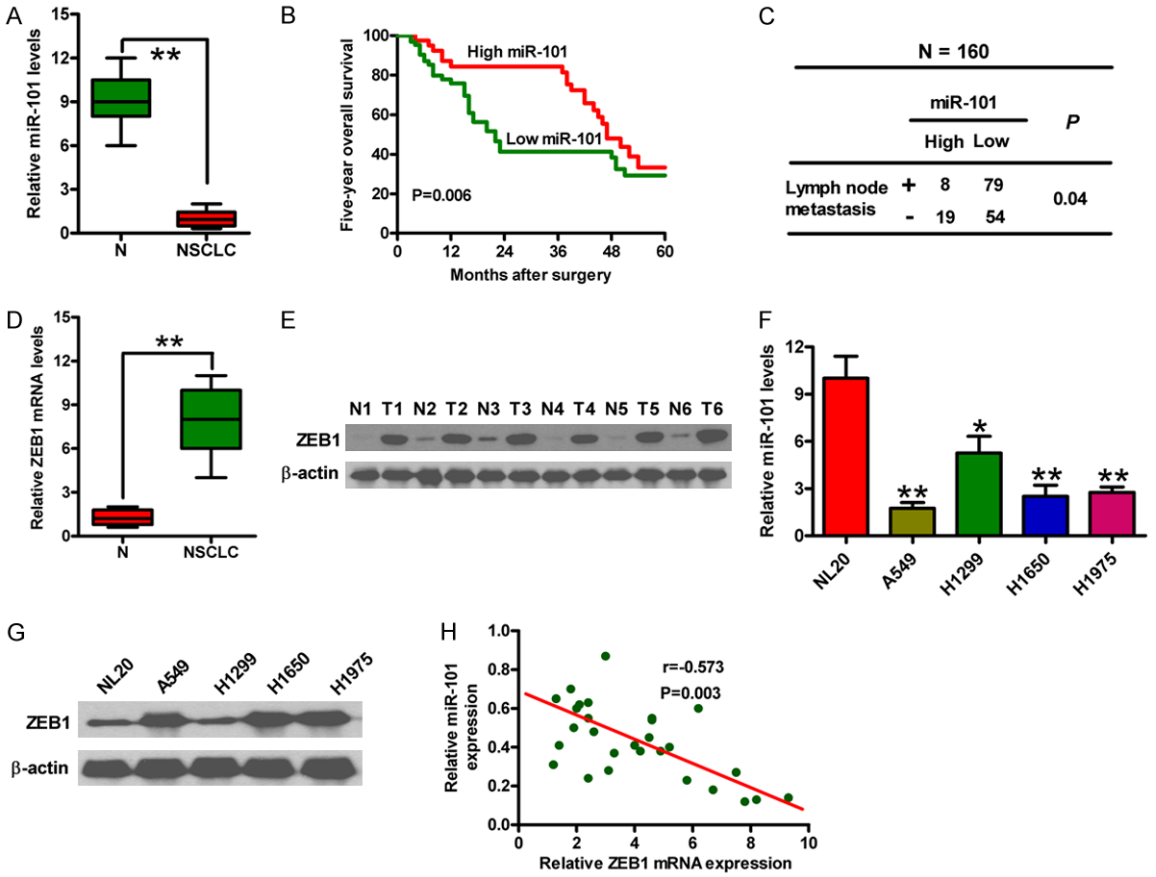

Figure 1. Expression levels of miR-101 and ZEB1 in NSCLC. A. qPCR analysis of miR-101 levels in NSCLC specimens and adjacent non-cancerous specimens (n = 40). U6 was used as the endogenous control. B. Kaplan-Meier survival curves showed lower five-year overall survival rate of NSCLC patients with low miR-101 levels (n = 73) compared with individuals with high miR-101 expression (n = 87). C. The comparison of lymph node metastasis between NSCLC patients with low miR-101 levels (n = 73) and individuals with high miR-101 expression (n = 87). D and E. qPCR (D) and Western blot (E) analyses of the mRNA and protein levels of ZEB1 in NSCLC specimens and the adjacent non-cancerous specimens. GAPDH and β-actin were used as the internal controls, respectively. F and G. qPCR (F) and Western blot (G) assays were performed to assess the relative expression of miR-101 and ZEB1 in normal lung epithelial cell line NL20 and NSCLC cell lines (A549, H1299, H1650, and H1975). U6 and β-actin were used as the endogenous controls. H. Correlation of the ZEB1 level and miR-101 expression in NSCLC cells. Data are presented as the mean ± SD of three replicates. *P < 0.05; **P < 0.01 compared with N group in (A and D) or compared with NL20 cells in (F). N: adjacent non-cancerous specimens.

ch were infected with a recombinant lentivirus expressing a miR-101 precursor or shZEB1 or the control lentiviruses, to the hind flanks of SCID mice (n = 6). Tumor volumes were measured and calculated as follows: tumor volume = (width^2 × length)/2. Tumor growth was monitored in vivo by intraperitoneally injection of D-luciferin (Promega) at a dose of 150 mg/kg. Luciferase imaging of the xenografts at day 14 after implantation were captured using the Xenogen IVIS imaging system and analyzed by using Living Image software (Xenogen Corporation, Berkeley, CA, USA). At 6 weeks after inoculation, the mice were sacrificed by euthanasia, and the tumors were weighed. For in vivo metastasis assays, SCID mice were injected with 1 × 10^6 A549-luc cells infected with various lentiviruses via the tail vein. The mice were sacrificed by euthanasia at 8 weeks after injection. The lung tissues were removed, fixed, embedded in paraffin, serially sectioned, and subjected to hematoxylin and eosin staining (Sigma). The metastases per section were counted.

Statistical analysis

Data are expressed as the mean ± standard derivation (SD). The statistical differences were determined by Student's two-tailed *t*-test for

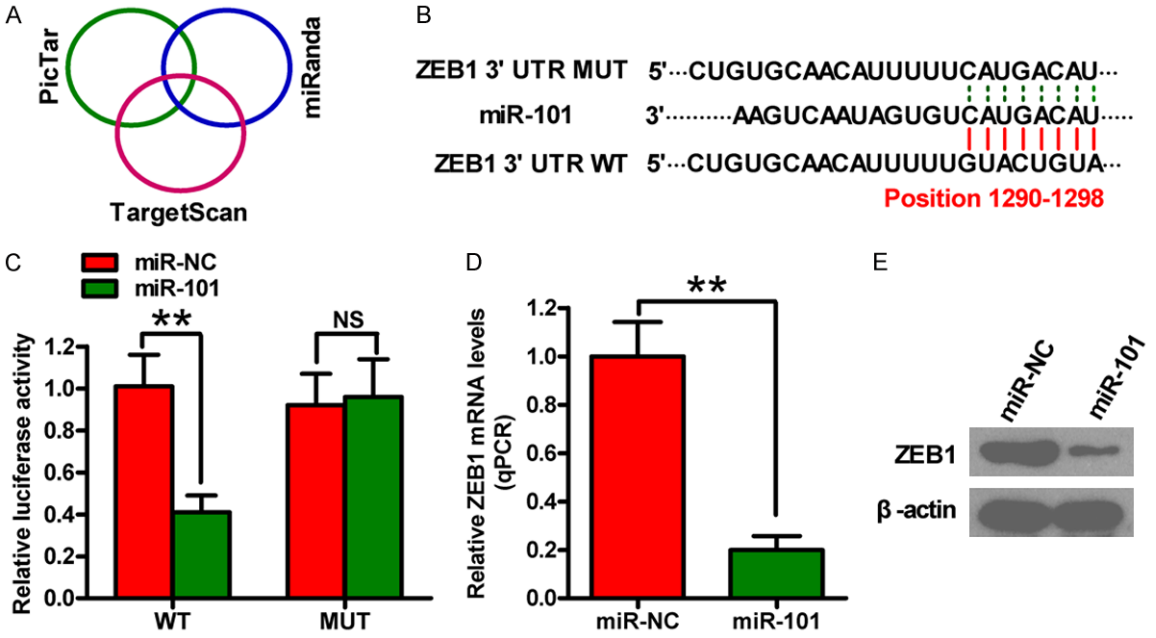

Figure 2. ZEB1 is a direct target of miR-101. A. Targetscan, PicTar, and miRanda were combinedly used to predict the potential targets of miR-101. B. 3'-UTR of ZEB1 was predicted to contain a complementary region of miR-101 seed sequences. C. Luciferase reporter plasmids harboring the WT or MUT 3'-UTR of ZEB1 were co-transfected with miR-NC or miR-101 mimics into A549 cells. Luciferase reporter assays were performed at 24 h after co-transfection. The normalized luciferase activity in the group (miR-NC + the empty plasmid) was set to 1. D and E. (D) mRNA and (E) protein levels of ZEB1 were assessed by qPCR and Western blot analyses in A549 cells transfected with miR-NC or miR-101. Data are presented as the mean ± SD of three replicates. **P < 0.01 compared with miR-NC group.

two groups and one-way analysis of variance among multiple groups. Chi-squared tests were used to evaluate the observed frequencies. The Kaplan-Meier method was utilized to draw the survival curve, and the log-rank test was employed for survival analysis. SPSS version 16.0 software (SPSS Inc., Chicago, IL, USA) was applied for statistical analyses. $P < 0.05$ was considered statistically significant.

Results

MiR-101 is lowly expressed and inversely correlated with ZEB1 expression in NSCLC tissues and cell lines

To analyze the role of miR-101 in NSCLC, we first detected miR-101 level in 20 pairs of NSCLC tissue specimens and the corresponding adjacent non-cancerous specimens using qPCR assay. **Figure 1A** shows lower miR-101 expression in the NSCLC tissues than in normal tissues. NSCLC patients with low levels of miR-101 had poor survival (**Figure 1B**) and high lymph node metastasis (**Figure 1C**) compared to the patients with high miR-101 levels. Next, we measured mRNA and protein expressions of ZEB1 in NSCLC tissues and the matched non-cancerous specimens. ZEB1 was highly expressed at both mRNA and protein levels in NSCLC tissues (**Figure 1D** and **1E**). Also, downregulation of miR-101 and upregulation of ZEB1 were observed in all NSCLC cells lines (A549, H1299, H1650, and H1975) compared with the normal lung bronchial epithelial cells line NL20 (**Figure 1F** and **1G**). The A549 cell line was selected for further studies because it had the lowest miR-101 level among all the tested NSCLC cell lines. Moreover, the levels of miR-101 and ZEB1 were inversely correlated in NSCLC cells (**Figure 1H**). These data implied that miR-101 and ZEB1 may play important roles in NSCLC.

MiR-101 directly targets ZEB1 in NSCLC cells

We applied three algorithms (TargetScan, miRanda, and PicTar) to search the candidate target genes of miR-101 (**Figure 2A**). The 3'-UTR of ZEB1 (1290–1298 nt) was found to contain a complementary region of miR-101 seed sequences (**Figure 2B**). Dual-luciferase reporter assays revealed that the introduction of miR-101 to A549 cells could suppress luciferase activity of the reporter plasmid with ZEB1-3'-

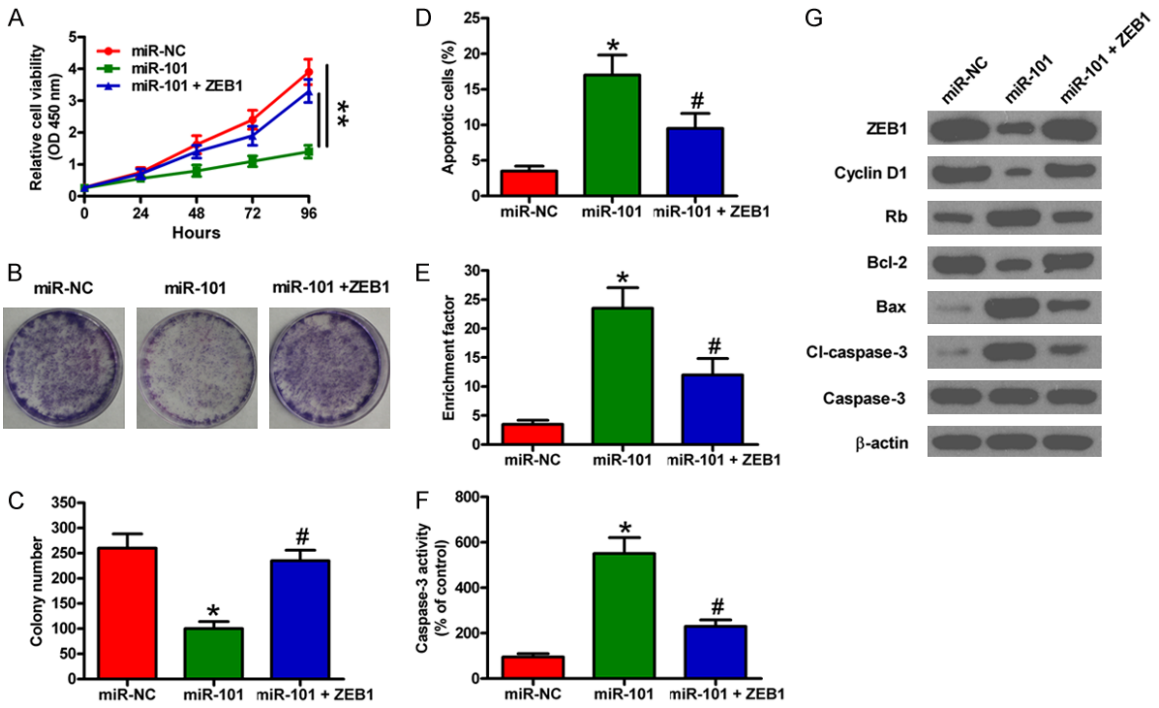

Figure 3. Suppression of proliferation and apoptosis resistance by miR-101 is mediated by ZEB1 in NSCLC cells. A549 cells were transfected with miR-NC, miR-101 mimics, or miR-101 + ZEB1-expressing plasmid. A. Cell viability was measured by MTT assay at 24, 48, 72, and 96 h after transfection. B. Colony formation assay was conducted to evaluate cell proliferation. C. The number of colonies in (B) was calculated. D. Cell apoptosis was analyzed by flow cytometry. The percentage of apoptotic cells was calculated. E. Cell apoptosis was measured by enrichment factor assay. F. Caspase-3 activity was measured to determine cell apoptosis. G. Representative results of Western blot showed the expression of ZEB1, Cyclin D1, Rb, Bcl-2, Bax, cl-caspase-3, and caspase-3. β-actin was used as the endogenous control. Data are presented as the mean ± SD of three replicates. *P < 0.05, **P < 0.01 compared with miR-NC group; #P < 0.05 compared with miR-101 group.

UTR-WT but did not limit the expression of a reporter fused to ZEB1-3'-UTR-MUT (**Figure 2C**). QPCR and Western blot analyses further confirmed that the miR-101 reduced ZEB1 mRNA and protein expressions in A549 cells (**Figure 2D** and **2E**). These results suggested that miR-101 directly targeted ZEB1 in NSCLC cells.

Inhibition of cell proliferation and apoptosis resistance by miR-101 is counteracted by ZEB1 overexpression in NSCLC cells

We investigated whether ZEB1 is a functional target of miR-101 in NSCLC. As shown in **Figure 3A**, the viability of miR-101-transfected A549 cells was significantly reduced compared with the miR-NC-transfected cells, which was attenuated by ZEB1 overexpression. Colony formation assay demonstrated that restoration of ZEB1 counteracted miR-101-inhibited A549 cell proliferation (**Figure 3B** and **3C**). Flow cytometry results showed a significant increase in apoptotic cells with miR-101 transfection. However, ZEB1 overexpression led to reduction of apoptotic cells (**Figure 3D**). Similar apoptosis was observed by enrichment factor and caspase-3 activity assays (**Figure 3E** and **3F**). Mechanistically, miR-101 markedly decreased the pro-survival Cyclin D1 and Bcl-2 expression but increased the levels of pro-apoptotic Bax and cl-caspase-3. However, the restored ZEB1 reversed the expression of the molecules mentioned above (**Figure 3G**). These findings indicated that miR-101 inhibited cell proliferation and apoptosis resistance by targeting ZEB1 in NSCLC in vitro.

Overexpression of ZEB1 counteracts the inhibitory effects of miR-101 on the migration and invasion of NSCLC cells

Next, we probed whether the inhibition of cell motility by miR-101 was mediated by ZEB1 in NSCLC. Wound-healing assay showed that miR-101 resulted in slow wound closure compared with miR-NC group, whereas ZEB1 restoration

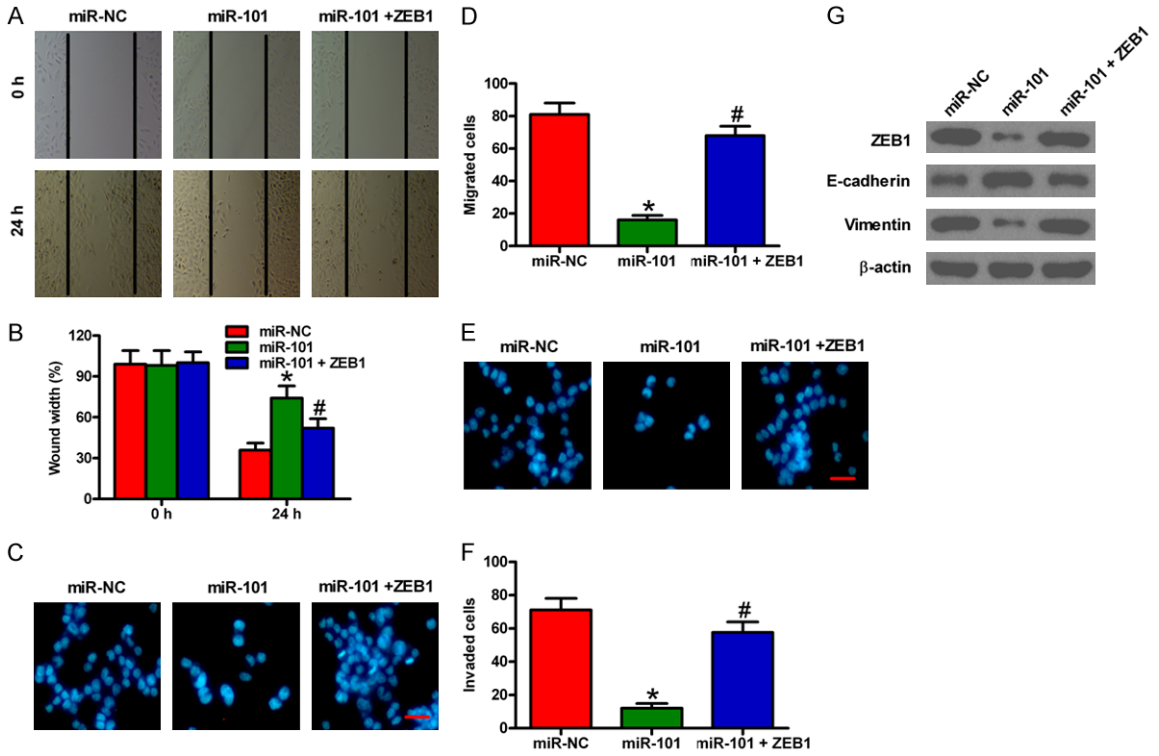

Figure 4. Inhibitory effects of miR-101 on migration and invasion are mediated by ZEB1 in NSCLC cells. A549 cells were transfected with miR-NC, miR-101 mimics, or miR-101 + ZEB1-expressing plasmid. (A) Wound-healing assay was performed to assess the migratory ability. (B) The wound width in (A) was measured. (C and E) Cell migration (C) and invasion (E) were evaluated by Transwell assays. (D and F) The numbers of migrated cells in (C) and invaded cells in (E) were calculated. (G) Representative results of Western blot showed the expression of ZEB1, E-cadherin and Vimentin. β-actin was used as the endogenous control. Data are presented as the mean ± SD of three replicates. *P < 0.05 compared with miR-NC group; #P < 0.05 compared with miR-101 group.

increased the migratory ability of A549 cells (**Figure 4A** and **4B**). Moreover, ZEB1 overexpression counteracted the migrated inhibition of A549 cells by miR-101 (**Figure 4C** and **4D**). Analogously, the invasion of A549 cells reduced by miR-101 was increased by ZEB1 overexpression (**Figure 4E** and **4F**). Mechanistically, miR-101 upregulated E-cadherin and downregulated vimentin in A549 cells, whereas ZEB1 reversed the expression of these two molecules (**Figure 4G**). These data confirmed that ZEB1 was a functional mediator of the repressive effects of miR-101 on the motility of NSCLC cells.

MiR-101 suppresses tumorigenesis and metastasis of NSCLC in vivo

To further investigate the biological role of miR-101 in vivo, xenograft or metastasis mouse model was established by subcutaneous or venous injection of A549-luc cells stably expressing miR-101 precursor or shZEB1. MiR-101 introduction or ZEB1 knockdown significantly retarded tumor growth (**Figure 5A**). miR-101 or shZEB1 group exhibited smaller tumor volumes and lighter tumor weights than control groups (**Figure 5B** and **5C**). TUNEL assay showed increased apoptotic cells in miR-101 overexpression or ZEB1 silencing groups (**Figure 5D**). In vivo lung metastases assay demonstrated that miR-101 restoration or ZEB1 depletion led to fewer metastatic nodules (**Figure 5E**). These results revealed that the inhibition of tumor growth and lung metastasis by miR-101 was mediated by ZEB1 in vivo.

Discussion

In this study, we found that miR-101 functioned as a tumor suppressor of NSCLC by targeting ZEB1. The key findings were as follows: first, miR-101 was significantly underexpressed in NSCLC tissues and cell lines. Second, miR-101 expression was inversely correlated with ZEB1 expression, as well as metastasis and poor survival rate in NSCLC patients. Third, miR-101 directly targeted ZEB1. Fourth, miR-101 restora-

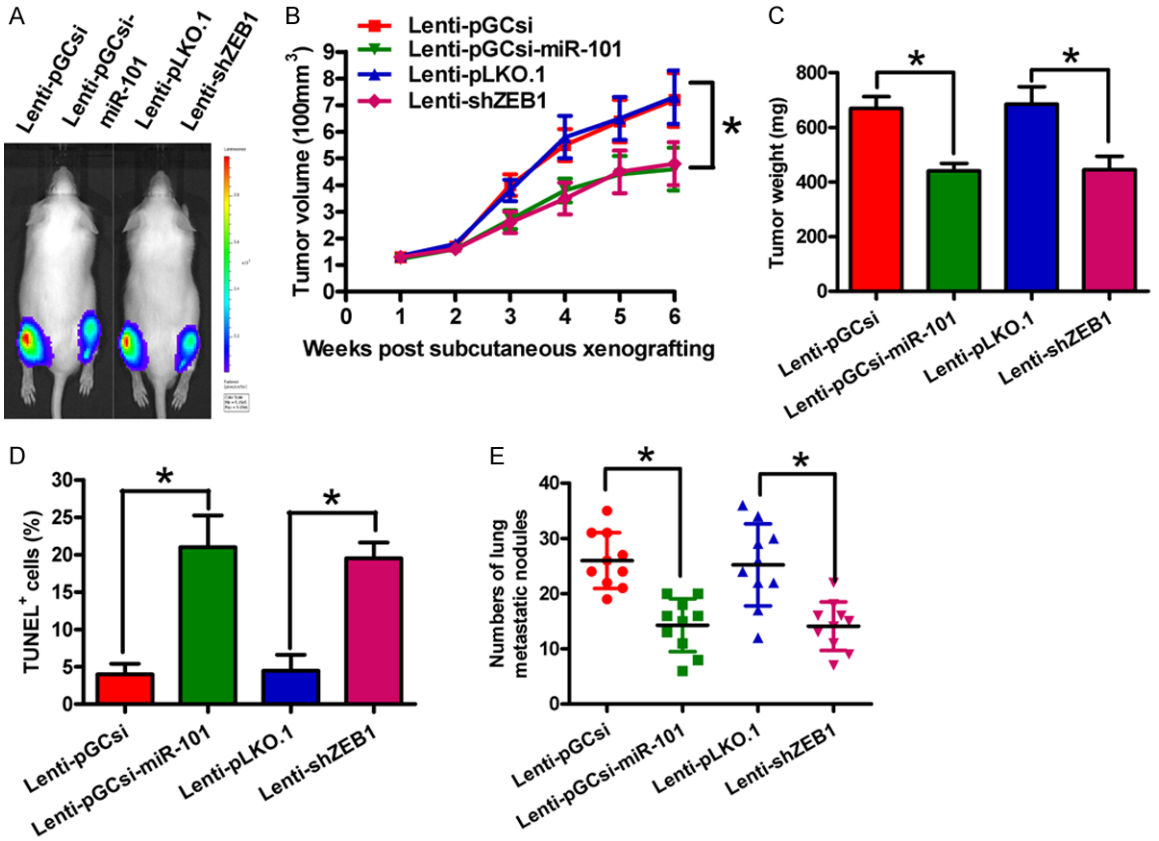

Figure 5. Overexpression of miR-101 or ZEB1 depletion retarded NSCLC growth and metastases in vivo. SCID mice were injected subcutaneously or via the tail vein with A549-luc cells infected with a control lentivirus (Lenti-pGCsi or Lenti-pLKO.1) or a recombinant lentivirus expressing a miR-101 precursor (Lenti-pGCsi-miR-101) or shZEB1 (Lenti-shZEB1). A. Tumor growth was measured by in vivo luciferase imaging of the xenografts 14 d after implantation. B. Tumor volume at 6 weeks after subcutaneous injection. C. Quantification of tumor weight at 8 weeks after xenografting. D. Cell apoptosis of the tumor tissues was detected by TUNEL assay. The percentage of TUNEL-positive cells was calculated. E. Quantification of microscopic nodules in the lungs of each group at 8 weeks after venous injection. Data are presented as the mean ± SD of three replicates. *P < 0.05 compared with Lenti-pGCsi or Lenti-pLKO.1 group.

tion inhibited NSCLC cell proliferation, apoptosis resistance, migration, and invasion in vitro, and tumor growth and lung metastasis in vivo. Lastly, the inhibitory effects of miR-101 on malignant phenotypes of NSCLC were attenuated and mimicked by the overexpression and knockdown of ZEB1, respectively. Overall, these results suggest the potential diagnostic and prognostic roles of miR-101 in NSCLC and indicate that miR-101 is a tumor suppressor of NSCLC by targeting ZEB1.

MiRNAs possess several features that make them attractive candidates as new prognostic biomarkers and powerful tools for the early diagnosis of lung cancer [28]. MiR-101 has been shown to be underexpressed and to act as a tumor suppressor in multiple cancers [13-16]. In the current study, we found that miR-101 was lowly expressed in NSCLC tissues and cell lines. NSCLC patients with high miR-101 levels generally had longer survival than patients with low miR-101 expression had, indicating the prognostic significance of miR-101 in NSCLC. Several studies have revealed that miR-101 may target multiple effectors to inhibit the tumorigenesis and metastasis of malignancies [13-16]. Here, we demonstrated that the ectopic expression of miR-101 reduced NSCLC cell proliferation, apoptosis resistance, migration, and invasion in vitro, and tumor growth and lung metastasis in vivo.

The relevance of ZEB1 to tumor progression has been studied in several human cancers [14, 18, 19]. In this study, we found that ZEB1

was significantly upregulated in NSCLC tissues and cell lines and inversely correlated with miR-101 level. A recent study has shown that targeting ZEB1 can inhibit colorectal cancer cell proliferation [29]. Majid et al. [30] reported that the knockdown of ZEB1 suppresses proliferation, migration, and invasion of bladder cancer cells and induces their apoptosis. As shown here, ZEB1 was directly targeted by tumor suppressor miR-101 in NSCLC. Furthermore, the overexpression and silencing of ZEB1 attenuated and mimicked, respectively, the inhibitory effects of miR-101 on NSCLC cell proliferation, apoptosis resistance, migration, and invasion in vitro, and tumor growth and lung metastasis in vivo, indicating that the inhibitory effects of miR-101 on malignant phenotypes of NSCLC are partly mediated by ZEB1 depletion.

Cyclin D1 can induce Rb phosphorylation and inactivation to promote G1/S phase transition [31]. Downregulation of cyclin D1 leads to conversion of Rb protein to the unphosphorylated form in A549 cells [32]. The apoptosis pathway is extensively regulated by the Bcl-2 family including pro-apoptotic Bax and anti-apoptotic factors Bcl-2 [33]. An increased Bax/Bcl-2 ratio can activates caspase-3, which is a major apoptotic executor, ultimately leading to cell apoptosis [34]. ZEB1 mediates miR-204-triggered the apoptosis of prostate cancer cells [35]. E-cadherin and vimentin are the significant hallmarks of EMT, which play important roles in the metastasis of lung cancer [36]. As a well-known transcriptional suppressor of E-cadherin, ZEB1 is reported to promote tumor invasion and metastasis by inducing EMT in cancer cells [37]. Zhang et al. [21] demonstrated that upregulation of ZEB1 is conversely correlated with E-cadherin expression and ZEB1 knockdown reduces the invasive ability of lung squamous cell carcinoma by increasing E-cadherin expression and decreasing vimentin level. Mechanistically, we here revealed that miR-101 significantly increased apoptosis-associated protein (Rb, Bax, and cl-caspase-3) expression and epithelial marker E-cadherin level, but decreased protein expression of proliferative cyclin D1, anti-apoptotic Bcl-2 and mesenchymal marker vimentin, which were reversed by ZEB1 overexpression, implying that miR-101 confers oncostatic roles by modulating the expression ZEB1 downstream molecules.

In summary, we demonstrated that miR-101 is lowly expressed in NSCLC tissues and cell lines and inversely correlated with ZEB1 expression, lymph-node metastasis, and poor prognosis of NSCLC patients. In vitro and in vivo assays showed that miR-101 retarded NSCLC growth and metastasis by targeting ZEB1. Therefore, miR-101 may be a potential therapeutic target for NSCLC.

Acknowledgements

This work was partly supported by Scientific Research Foundation of Shaanxi Health and Family Planning Committee (No.2016E003).

Disclosure of conflict of interest

None.

Address correspondence to: Dr. Tao Jiang, Department of Thoracic Surgery, Tangdu Hospital, The Fourth Military Medical University, No.1 Xinsi Road, Xi'an 710038, Shannxi, China. Tel: +86-29-84777556; Fax: +86-29-84777556; E-mail: jiangtaofmmu@163.com

References

[1] Siegel R, Ma J, Zou Z and Jemal A. Cancer statistics, 2014. CA Cancer J Clin 2014; 64: 9-29.
[2] Ferlay J, Soerjomataram I, Dikshit R, Eser S, Mathers C, Rebelo M, Parkin DM, Forman D and Bray F. Cancer incidence and mortality worldwide: sources, methods and major patterns in GLOBOCAN 2012. Int J Cancer 2015; 136: E359-386.
[3] Chen W, Zheng R, Baade PD, Zhang S, Zeng H, Bray F, Jemal A, Yu XQ and He J. Cancer statistics in China, 2015. CA Cancer J Clin 2016; 66: 115-132.
[4] Herbst RS, Heymach JV and Lippman SM. Lung cancer. N Engl J Med 2008; 359: 1367-1380.
[5] Shepherd FA, Douillard JY and Blumenschein GR Jr. Immunotherapy for non-small cell lung cancer: novel approaches to improve patient outcome. J Thorac Oncol 2011; 6: 1763-1773.
[6] Zamore PD and Haley B. Ribo-gnome: the big world of small RNAs. Science 2005; 309: 1519-1524.
[7] Valencia-Sanchez MA, Liu J, Hannon GJ and Parker R. Control of translation and mRNA degradation by miRNAs and siRNAs. Genes Dev 2006; 20: 515-524.
[8] Calin GA and Croce CM. MicroRNA signatures in human cancers. Nat Rev Cancer 2006; 6: 857-866.
[9] Del Vescovo V and Denti MA. microRNA and lung cancer. Adv Exp Med Biol 2015; 889: 153-177.

[10] Liu F, Song D, Wu Y, Liu X, Zhu J and Tang Y. MiR-155 inhibits proliferation and invasion by directly targeting PDCD4 in non-small cell lung cancer. Thorac Cancer 2017; 8: 613-619.
[11] Liu XH, Lu KH, Wang KM, Sun M, Zhang EB, Yang JS, Yin DD, Liu ZL, Zhou J, Liu ZJ, De W and Wang ZX. MicroRNA-196a promotes non-small cell lung cancer cell proliferation and invasion through targeting HOXA5. BMC Cancer 2012; 12: 348.
[12] Miao LJ, Huang SF, Sun ZT, Gao ZY, Zhang RX, Liu Y and Wang J. MiR-449c targets c-Myc and inhibits NSCLC cell progression. FEBS Lett 2013; 587: 1359-1365.
[13] Li JT, Jia LT, Liu NN, Zhu XS, Liu QQ, Wang XL, Yu F, Liu YL, Yang AG and Gao CF. MiRNA-101 inhibits breast cancer growth and metastasis by targeting CX chemokine receptor 7. Oncotarget 2015; 6: 30818-30830.
[14] Wu B, Lei D, Wang L, Yang X, Jia S, Yang Z, Shan C, Yang X, Zhang C and Lu B. MiRNA-101 inhibits oral squamous-cell carcinoma growth and metastasis by targeting zinc finger E-box binding homeobox 1. Am J Cancer Res 2016; 6: 1396-1407.
[15] Ye Z, Yin S, Su Z, Bai M, Zhang H, Hei Z and Cai S. Downregulation of miR-101 contributes to epithelial-mesenchymal transition in cisplatin resistance of NSCLC cells by targeting ROCK2. Oncotarget 2016; 7: 37524-37535.
[16] Zhang JG, Guo JF, Liu DL, Liu Q and Wang JJ. MicroRNA-101 exerts tumor-suppressive functions in non-small cell lung cancer through directly targeting enhancer of zeste homolog 2. J Thorac Oncol 2011; 6: 671-678.
[17] Onder TT, Gupta PB, Mani SA, Yang J, Lander ES and Weinberg RA. Loss of E-cadherin promotes metastasis via multiple downstream transcriptional pathways. Cancer Res 2008; 68: 3645-3654.
[18] Zhou YM, Cao L, Li B, Zhang RX, Sui CJ, Yin ZF and Yang JM. Clinicopathological significance of ZEB1 protein in patients with hepatocellular carcinoma. Ann Surg Oncol 2012; 19: 1700-1706.
[19] Shen A, Zhang Y, Yang H, Xu R and Huang G. Overexpression of ZEB1 relates to metastasis and invasion in osteosarcoma. J Surg Oncol 2012; 105: 830-834.
[20] Ren J, Chen Y, Song H, Chen L and Wang R. Inhibition of ZEB1 reverses EMT and chemoresistance in docetaxel-resistant human lung adenocarcinoma cell line. J Cell Biochem 2013; 114: 1395-1403.
[21] Zhang J, Lu C, Zhang J, Kang J, Cao C and Li M. Involvement of ZEB1 and E-cadherin in the invasion of lung squamous cell carcinoma. Mol Biol Rep 2013; 40: 949-956.
[22] Aigner K, Dampier B, Descovich L, Mikula M, Sultan A, Schreiber M, Mikulits W, Brabletz T, Strand D, Obrist P, Sommergruber W, Schweifer N, Wernitznig A, Beug H, Foisner R and Eger A. The transcription factor ZEB1 (deltaEF1) promotes tumour cell dedifferentiation by repressing master regulators of epithelial polarity. Oncogene 2007; 26: 6979-6988.
[23] Funahashi J, Sekido R, Murai K, Kamachi Y and Kondoh H. Delta-crystallin enhancer binding protein delta EF1 is a zinc finger-homeodomain protein implicated in postgastrulation embryogenesis. Development 1993; 119: 433-446.
[24] Son H and Moon A. Epithelial-mesenchymal transition and cell invasion. Toxicol Res 2010; 26: 245-252.
[25] Wang J, Zhou F, Yin L, Zhao L, Zhang Y and Wang J. MicroRNA-199b targets the regulation of ZEB1 expression to inhibit cell proliferation, migration and invasion in nonsmall cell lung cancer. Mol Med Rep 2017; 16: 5007-5014.
[26] Li YJ, Ping C, Tang J and Zhang W. MicroRNA-455 suppresses non-small cell lung cancer through targeting ZEB1. Cell Biol Int 2016; 40: 621-628.
[27] Zhang HY, Zheng FS, Yang W and Lu JB. The long non-coding RNA MIAT regulates zinc finger E-box binding homeobox 1 expression by sponging miR-150 and promoteing cell invasion in non-small-cell lung cancer. Gene 2017; 633: 61-65.
[28] Joshi P, Middleton J, Jeon YJ and Garofalo M. MicroRNAs in lung cancer. World J Methodol 2014; 4: 59-72.
[29] Quan Y, Xu M, Cui P, Ye M, Zhuang B and Min Z. Grainyhead-like 2 promotes tumor growth and is associated with poor prognosis in colorectal cancer. J Cancer 2015; 6: 342-350.
[30] Majid S, Dar AA, Saini S, Deng G, Chang I, Greene K, Tanaka Y, Dahiya R and Yamamura S. MicroRNA-23b functions as a tumor suppressor by regulating Zeb1 in bladder cancer. PLoS One 2013; 8: e67686.
[31] Obaya AJ and Sedivy JM. Regulation of cyclin-Cdk activity in mammalian cells. Cell Mol Life Sci 2002; 59: 126-142.
[32] Alteri A, De Vito F, Messina G, Pompili M, Calconi A, Visca P, Mottolese M, Presutti C and Grossi M. Cyclin D1 is a major target of miR-206 in cell differentiation and transformation. Cell Cycle 2013; 12: 3781-3790.
[33] Adams JM and Cory S. The Bcl-2 apoptotic switch in cancer development and therapy. Oncogene 2007; 26: 1324-1337.
[34] Redza-Dutordoir M and Averill-Bates DA. Activation of apoptosis signalling pathways by reactive oxygen species. Biochim Biophys Acta 2016; 1863: 2977-2992.

[35] Wu G, Wang J, Chen G and Zhao X. microRNA-204 modulates chemosensitivity and apoptosis of prostate cancer cells by targeting zinc-finger E-box-binding homeobox 1 (ZEB1). Am J Transl Res 2017; 9: 3599-3610.

[36] Ma K, Fan Y, Dong X, Dong D, Guo Y, Wei X, Ning J, Geng Q, Wang C, Hu Y, Li M, Niu W, Li E and Wu Y. MTA1 promotes epithelial to mesenchymal transition and metastasis in non-small-cell lung cancer. Oncotarget 2017; 8: 38825-38840.

[37] Zhang P, Sun Y and Ma L. ZEB1: at the crossroads of epithelial-mesenchymal transition, metastasis and therapy resistance. Cell Cycle 2015; 14: 481-487.